Inorg. Chem. **2007**, *46*, 7477–7488

Systematic Studies of Early Actinide Complexes: Uranium(IV) Fluoroketimides

Eric J. Schelter, Ping Yang, Brian L. Scott, J. D. Thompson, Richard L. Martin, P. Jeffrey Hay,* David E. Morris,* and Jaqueline L. Kiplinger*

Los Alamos National Laboratory, Los Alamos, New Mexico 87545

Received March 8, 2007

The reaction of $(C_5Me_5)_2U(CH_3)_2$ with 2 equiv of $N{\equiv}C{-}Ar_F$ gives the fluorinated uranium(IV) bis(ketimide) complexes $(C_5Me_5)_2U[{-}N{=}C(CH_3)(Ar_F)]_2$ [where Ar_F = 2-F-C_6H_4 (**4**), 3-F-C_6H_4 (**5**), 4-F-C_6H_4 (**6**), 2,6-F_2-C_6H_3 (**7**), 3,5-F_2-C_6H_3 (**8**), 2,4,6-F_3-C_6H_2 (**9**), 3,4,5-F_3-C_6H_2 (**10**), and C_6F_5 (**11**)]. These have been characterized by single-crystal X-ray diffraction, ^{1}H and ^{19}F NMR, cyclic voltammetry, UV–visible–near-IR absorption spectroscopy, and variable-temperature magnetic susceptibility. Density functional theory (DFT) results are reported for complexes **6** and **11** for comparison with experimental data. The most significant structural perturbation imparted by the F substitution in these complexes is a rotation of the fluorinated aryl (Ar_F) group out of the plane defined by the $N{=}C(C_{Me})(C_{ipso})$ fragment in complexes **7**, **9**, and **11** when the Ar_F group possesses two *o*-fluorine atoms. Excellent agreement is obtained between the DFT-calculated and experimental crystal structures for **11**, which displays the distortion, as well as for **6**, which does not. In **7**, **9**, and **11**, the out-of-plane rotation results in large angles (ϕ = 53.7–89.4°) between the planes formed by ketimide atoms $N{=}C(C_{Me})(C_{ipso})$ and the ketimide aryl groups. Complexes **6** and **10** do not contain *o*-fluorine atoms and display interplanar angles in the range of ϕ = 7–26.8°. Complex **4** with a single *o*-fluorine substituent has intermediate values of ϕ = 20.4 and 49.5°. The distortions in **7**, **9**, and **11** result from an unfavorable steric interaction between one of the two *o*-fluorine atoms and the methyl group [$-N{=}C(CH_3)$] on the ketimide ligand. All complexes exhibit U^V/U^{IV} and U^{IV}/U^{III} redox couples, although the distortion in **7**, **9**, and **11** appears to be a factor in rendering the U^{IV}/U^{III} couple irreversible. The potential separation between these couples remains constant at 2.15 ± 0.03 V. The electronic spectra are dominated by unusually intense f–f transitions in the near-IR that retain nearly identical band energies but vary in intensity as a function of the fluorinated ketimide ligand, and visible and near-UV bands assigned to metal (5f)-to-ligand (π^*) charge-transfer and interconfiguration ($5f^2 \rightarrow 5f^1$-$6d^1$) transitions, respectively. Variable-temperature magnetic susceptibility data for these complexes indicate a temperature-independent paramagnetism (TIP) below ∼50 K that results from admixing of low-lying crystal-field excited states derived from the symmetry-split $^3H_4$ $5f^2$ manifold into the ground state. The magnitude of the TIP is smaller for the complexes possessing two *o*-fluorine atoms (**7**, **9**, and **11**), indicating that the energy separation between ground and TIP-admixed excited states is larger as a consequence of the greater basicity of these ligands.

Introduction

Complexes of the light actinide elements (Th−Pu) present an important challenge in understanding electronic structure and bonding because they frequently defy the conventions established for both the transition metals and the lanthanides. Our group has been using organometallic Th and U complexes as tunable platforms for systematically studying the electronic structure of early actinides.[1−4] Specifically, studies on the uranium(IV) bis(ketimide) complexes $(C_5Me_5)_2U[{-}N{=}C(Ph)(R)]_2$ [R = Ph (**1**), CH_2Ph (**2**), CH_3 (**3**)] have shown

* To whom correspondence should be addressed. E-mail: pjhay@lanl.gov (P.J.H.), demorris@lanl.gov (D.E.M.), kiplinger@lanl.gov (J.L.K.).

(1) Morris, D. E.; Da Re, R. E.; Jantunen, K. C.; Castro-Rodriguez, I.; Kiplinger, J. L. *Organometallics* **2004**, *23*, 5142.
(2) Schelter, E. J.; Yang, P.; Hay, P. J.; Martin, R. L.; Scott, B. L.; Da Re, R. E.; Jantunen, K. C.; Morris, D. E.; Kiplinger, J. L. *J. Am. Chem. Soc.* **2007**, *129*, 5139.
(3) Kiplinger, J. L.; Pool, J. A.; Schelter, E. J.; Thompson, J. D.; Scott, B. L.; Morris, D. E. *Angew. Chem., Int. Ed.* **2006**, *45*, 2036.
(4) Schelter, E. J.; Veauthier, J. M.; Thompson, J. D.; Scott, B. L.; John, K. D.; Morris, D. E.; Kiplinger, J. L. *J. Am. Chem. Soc.* **2006**, *128*, 2198.

10.1021/ic700455b CCC: $37.00
Published on Web 08/11/2007

numerous spectroscopic signatures typically associated with transition-metal complexes including charge-transfer (CT) transitions, enhancements in the intensity of ligand-field transitions presumably from coupling to these CT states, and enhancement in the Raman vibrational spectrum when excited in resonance with the CT and ligand-localized electronic excited states.[1,5] Notably, the metal-based orbitals

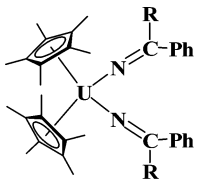

R = Ph (**1**), CH_2Ph (**2**), CH_3 (**3**)

involved in all of these electronic transitions appear to be principally 5f in character, and the implication is that these spectral signatures arise because of significant covalent interactions between the 5f orbitals and those on the ketimide ligands.

These intriguing spectroscopic results prompted us to explore in greater detail archetypical transition-metal electronic structure concepts in these actinide systems through the preparation and characterization of a more extensive series of structurally homologous but electronically diverse uranium(IV) complexes. Recently, we described the synthesis, structures, electrochemistry, and electronic spectroscopy (including novel luminescent behavior) for a series of fluorinated $5f^06d^0$ thorium(IV) bis(ketimide) complexes.[2] This study was also supported by theoretical calculations of optimized molecular and electronic structures. In the present report, we investigate the analogous series of fluorinated uranium bis(ketimide) complexes $(C_5Me_5)_2U[-N{=}C(CH_3)(Ar_F)]_2$ [where Ar_F = 2-F-C_6H_4 (**4**), 3-F-C_6H_4 (**5**), 4-F-C_6H_4 (**6**), 2,6-F_2-C_6H_3 (**7**), 3,5-F_2-C_6H_3 (**8**), 2,4,6-F_3-C_6H_2 (**9**), 3,4,5-F_3-C_6H_2 (**10**), and C_6F_5 (**11**)] with particular attention to unraveling the added complexities associated with the $5f^2$ valence electronic configuration in these U^{IV} species. These new results demonstrate clear ligand-based substituent effects that have allowed for tuning of the covalent signatures and the degree of metal−ligand multiple bonding in a series of uranium(IV) ketimide complexes.

Experimental Section

Instrumentation and Sample Protocols. Electronic absorption spectral data were obtained for toluene and tetrahydrofuran (THF) solutions of complexes over the wavelength range 300−1600 nm on a Perkin-Elmer model Lambda 950 UV−visible−near-IR spectrophotometer. All data were collected in 1 cm path length cuvettes loaded in a recirculating Vacuum Atmospheres model HE-553-2 inert atmosphere (N_2) drybox with a MO-40-2 Dri-Train and run versus a toluene or THF solvent reference. Samples were typically run at two dilutions, ∼0.1 and ∼0.5 mM, to optimize the absorbance in the UV−visible and near-IR, respectively. The spectral resolution was typically 2 nm in the visible region and 4−6 nm in the near-IR region.

Cyclic and square-wave voltammetric data were obtained in the Vacuum Atmospheres drybox system described above. All data were collected using a Perkin-Elmer Princeton Applied Research Corp. (PARC) model 263 potentiostat under computer control with PARC model 270 software. All sample solutions were ∼5 mM in complex with a 0.1 M $[Bu_4N][B(C_6F_5)_4]$ supporting electrolyte in THF solvent. The advantageous properties of this quarternary ammonium salt as an electrolyte for voltammetric studies in low-dielectric-constant solvents have been noted in several recent reports,[6,7] and the origin of this effect has recently been demonstrated to be directly related to the greater dissociation of the cation/anion pair in low-dielectric-constant media such as THF as a result of the more highly delocalized charge in the $[B(C_6F_5)_4]^-$ anion.[8] Furthermore, this anion appears to be more inert toward fluoride abstraction chemistry. All data were collected with the positive-feedback IR compensation feature of the software/potentiostat activated to ensure minimal contribution to the voltammetric waves from uncompensated solution resistance (typically ∼1 kΩ under the conditions employed). Solutions were contained in PARC model K0264 microcells consisting of a ∼3 mm diameter Pt disk working electrode, a Pt wire counter electrode, and a Ag wire quasi-reference electrode. Scan rates from 20 to 5000 mV/s were employed in the cyclic voltammetry scans to assess the chemical and electrochemical reversibility of the observed redox transformations. Half-wave potentials were determined from the peak values in the square-wave voltammograms or from the average of the cathodic and anodic peak potentials in the reversible cyclic voltammograms. Potential calibrations were performed at the end of each data collection cycle using the ferrocenium/ferrocene couple as an internal standard. Electronic absorption and cyclic voltammetric data were analyzed using Wavemetrics IGOR Pro (version 4.0) software on a Macintosh platform.

Synthesis. The syntheses of compounds $(C_5Me_5)_2U[-N{=}C(CH_3)(Ar_F)]_2$ [where Ar_F = 2-F-C_6H_4 (**4**), 3-F-C_6H_4 (**5**), 4-F-C_6H_4 (**6**), 2,6-F_2-C_6H_3 (**7**), 3,5-F_2-C_6H_3 (**8**), 2,4,6-F_3-C_6H_2 (**9**), 3,4,5-F_3-C_6H_2 (**10**), and C_6F_5 (**11**)] are similar to those previously reported for their thorium analogues and complexes **2** and **3**.[2,9] A generic procedure is reported here for complexes **4**−**11**. In an N_2 atmosphere drybox, a 125 mL flask equipped with a magnetic stirbar was charged with $(C_5Me_5)_2U(CH_3)_2$ and 60 mL of toluene. Toluene solutions of fluorinated nitrile were added to the red-orange $(C_5Me_5)_2U(CH_3)_2$ solutions, resulting in an immediate color change to dark red-brown, and the reaction mixture was stirred at room temperature for 12−15 h. The volatiles were then removed under reduced pressure to give solids. The solids were dissolved in pentane (50 mL) and the solutions filtered through a Celite-padded coarse frit. The filtrate was collected, the solvent removed using dynamic vacuum, and the resulting solid product collected. The final purifications varied slightly for each complex. See the Supporting Information for additional details.

Computational Details. The B3LYP hybrid density functional theory (DFT)[10] was employed to optimize the equilibrium molecular structures of **6**, **11**, and their anions. The pentamethylcyclopentadienyl (C_5Me_5) groups in the complexes were used in calculations

(5) Da Re, R. E.; Jantunen, K. C.; Golden, J. T.; Kiplinger, J. L.; Morris, D. E. *J. Am. Chem. Soc.* **2005**, *127*, 682.
(6) Camire, N.; Mueller-Westerhoff, U. T.; Geiger, W. E. *J. Organomet. Chem.* **2001**, *637*, 823.
(7) LeSuer, R. J.; Geiger, W. E. *Angew. Chem., Int. Ed.* **2000**, *39*, 248.
(8) LeSuer, R. J.; Buttolph, C.; Geiger, W. E. *Anal. Chem.* **2004**, *76*, 6395.
(9) Jantunen, K. C.; Burns, C. J.; Castro-Rodriguez, I.; Da Re, R. E.; Golden, J. T.; Morris, D. E.; Scott, B. L.; Taw, F. L.; Kiplinger, J. L. *Organometallics* **2004**, *23*, 4682.
(10) Becke, A. D. *J. Chem. Phys.* **1993**, *98*, 5648.

without simplification. The Stuttgart RSC 1997 ECP was employed for U, which incorporates scalar relativistic effects and replaces 60 core electrons.[11] The valence electrons were represented as [8s/7p/6d/4f], and 6-31G* basis sets were used for C, H, N, and F. All calculations were carried out with the *Gaussian03* suite of codes.[12] Natural orbital population analysis was carried out on the total electron density from the unrestricted DFT calculations.[12] The natural orbitals (NOs) with occupancies of 1.0 give the most compact representation of the unpaired spin density.

Results and Discussion

Structural Chemistry. Equation 1 presents the synthetic methods used and the yields obtained in the preparation of the fluorinated uranium(IV) ketimide complexes. The reaction of a red-orange toluene solution of $(C_5Me_5)_2U(CH_3)_2$ with 2 equiv of nitrile at room temperature produced the corresponding uranium(IV) bis(ketimide) complexes **4**−**11**. Following workup, all complexes were reproducibly isolated in pure form as brown solids despite the modest yields for some of them, which reflect the high solubility imparted by the fluorinated ligands. Single-crystal X-ray crystallography of compounds **4**, **6**, **7**, and **9**−**11** confirms the expected structures for these complexes, consistent with the ^{1}H and ^{19}F NMR data in all cases (Figure 1 and Supporting Information). Isolation of these species further demonstrates the compatibility of U and Th ions with fluorinated organic ligands.[2] Representative structures of **9** and **10** are shown in Figure 1, and the crystallographic parameters for **4**, **6**, **7**, and **9**−**11** are listed in Table 1. Table 2 presents salient geometric parameters for complexes **1**, **2**, **4**, **6**, **7**, and **9**−**11**. Single crystals were not obtained for **5** or **8**, but their formulations are consistent with their ^{1}H and ^{19}F NMR spectroscopic data (see the Supporting Information).

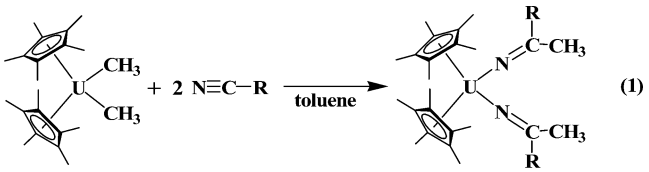

(1)

R = 2-F-C_6H_4 (**4**), 62 %
3-F-C_6H_4 (**5**), 61 %
4-F-C_6H_4 (**6**), 40 %
2,6-F_2-C_6H_3 (**7**), 31 %
3,5-F_2-C_6H_3 (**8**), 64 %
2,4,6-F_3-C_6H_2 (**9**), 59 %
3,4,5-F_3-C_6H_2 (**10**), 65 %
C_6F_5 (**11**), 79 %

The U−N distances observed for **4**, **6**, **7**, and **9**−**11** span from 2.169(9) to 2.220(3) Å and fall within the range observed for previously reported uranium(IV) ketimide complexes, 2.04(2)−2.225(5) Å.[9,13] Evidence for U−N bond orders slightly greater than 1 in complexes **4**, **6**, **7**, and **9**−**11** is deduced from a general shortening of these distances by

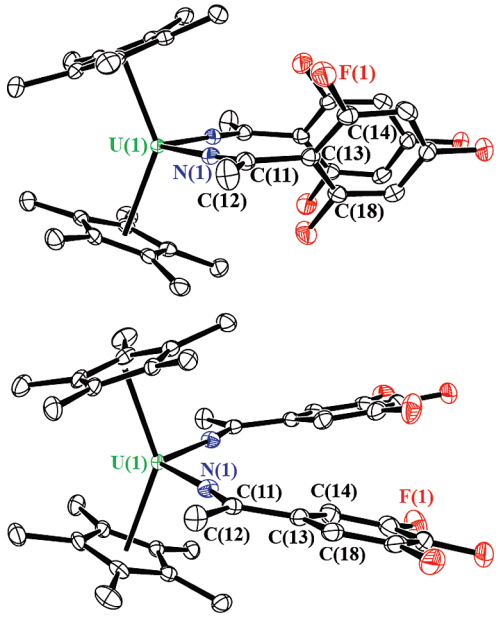

Figure 1. Thermal ellipsoid plots of **9** (top) and **10** (bottom) with ellipsoids projected at the 50% probability level. The U(1) atom resides on a crystallographically imposed inversion center. Coplanarity is observed in **10** for planes formed by the ketimide aryl groups and atoms N(1)−C(11)−C(12)−C(13), while in **9**, these planes are nearly orthogonal.

∼0.1 Å compared to structurally related uranium(IV) amide complexes, which possess canonical U−N single bonds [2.237(3)−2.267(6) Å],[14,15] while the structurally relevant uranium(IV) imido complex $(C_5Me_5)_2U(=N\text{-}2,4,6\text{-}{}^tBu_3C_6H_2)$ possesses a U=N bond length of 1.952(12) Å.[16] No obvious trends in the U−N distances for the $(C_5Me_5)_2U[-N=C(CH_3)(Ar_F)]_2$ complexes can be deduced on the basis of simple extent of fluorination or electron-withdrawing ability of the ketimide ligand substituents.

A primary structural effect was identified for the isostructural $(C_5Me_5)_2Th[-N=C(CH_3)(Ar_F)]_2$ systems, which apparently masks any anticipated trends among structure, bonding, and associated spectroscopic and electrochemical properties. Specifically, F substitution at both ortho positions of the ketimide aryl group [i.e., $(C_5Me_5)_2Th[-N=C(CH_3)(Ar_F)]_2$, where Ar_F = 2,6-F_2-C_6H_3, 2,4,6-F_3-C_6H_2, or C_6F_5] was found to produce an unfavorable steric interaction that forces the aryl group to be rotated approximately orthogonal to the plane formed by the $-N=C(C_{Me})(C_{ipso})$ atoms of the ketimide ligand and results in disruption of conjugation through the ketimide ligand. As illustrated for complexes **9** and **10** in Figure 1, this distortion is conveniently quantified by analyzing the torsion angles that describe the smallest interplanar angle formed by atoms N(1)−C(11)−C(13)−C(14/18). Looking down the C(11)−C(13) axis, out-of-plane distortions of the aryl ring result from either clockwise or counterclockwise rotation of the group along the C(11)−C(13) axis. The interplanar angles (ϕ) range from 0° [aryl groups planar to ketimide atoms $N=C(C_{Me})(C_{ipso})$] to 90°

(11) Kuchle, W.; Dolg, M.; Stoll, H.; Preuss, H. *J. Chem. Phys.* **1994**, *100*, 7535.
(12) Frisch, M. J.; Trucks, G. W.; Schlegel, H. B. *Gaussian03*, revision C.02; Gaussian, Inc.: Wallingford, CT, 2004.
(13) Kiplinger, J. L.; Morris, D. E.; Scott, B. L.; Burns, C. J. *Organometallics* **2002**, *21*, 3073.
(14) Straub, T.; Frank, W.; Reiss, G. J.; Eisen, M. S. *J. Chem. Soc., Dalton Trans.* **1996**, 2541.
(15) Peters, R. G.; Scott, B. L.; Burns, C. J. *Acta Crystallogr., Sect. C: Cryst. Struct. Commun.* **1999**, *55*, 1482.
(16) Arney, D. S. J.; Burns, C. J. *J. Am. Chem. Soc.* **1995**, *117*, 9448.

Table 1. Crystallographic Experimental Parameters for **4**, **6**, **7**, and **9**−**11**

	4	**6**	**7**	**9**	**10**	**11**
formula	$C_{36}H_{44}F_2N_2U$	$C_{36}H_{44}F_2N_2U$	$C_{36}H_{42}F_4N_2U$	$C_{36}H_{40}F_6N_2U$	$C_{36}H_{40}F_6N_2U$	$C_{36}H_{36}F_{10}N_2U$
a (Å)	10.0173(5)	17.9790(19)	10.6877(6)	13.5252(5)	12.9529(6)	15.9821(4)
b (Å)	17.6957(9)	18.0889(19)	17.5713(9)	14.5744(5)	13.8105(6)	16.3139(4)
c (Å)	18.322(1)	9.9044(11)	19.3511(10)	17.1466(6)	18.5471(8)	26.9285(6)
α (deg)	90	90	108.793(1)	90	90	90
β (deg)	90	90	90.476(1)	96.434(1)	99.7810(10)	90
γ (deg)	90	90	102.700(1)	90	90	90
V (Å^3)	3247.8(3)	3221.1(6)	3343.8(3)	3358.7(2)	3269.6(3)	7021.1(3)
Z	4	4	4	4	4	8
fw	780.76	780.76	816.75	852.73	852.73	924.70
space group	$P2_12_12_1$	*Pnma*	$P\bar{1}$	*C*2/*c*	*C*2/*c*	*Pccn*
T (K)	141(1)	141(1)	141(1)	141(1)	141(1)	141(1)
λ (Å)	0.710 73	0.710 73	0.710 73	0.710 73	0.710 73	0.710 73
D_{calcd} (g cm^{-3})	1.597	1.610	1.622	1.686	1.732	1.750
μ (mm^{-1})	5.035	5.077	4.903	4.893	5.027	4.705
R1 [$I > 2\sigma(I)$][a]	0.0316	0.0735	0.0286	0.0197	0.0182	0.0318
wR2 (all data)[b]	0.0694	0.1960	0.0689	0.0501	0.0498	0.1002

Table 2. Geometric Parameters for **1**, **2**, **4**, **6**, **7**, and **9**−**11**

	1	**2**	**4**	**6**	**7**	**9**	**10**	**11**
U−N (Å)	2.184(5)	2.184(3)	2.196(4)	2.169(9)	2.185(3)	2.193(2)	2.1974(18)	2.204(5)
	2.203(6)		2.200(4)		2.220(3)			2.199(5)
	2.185(5)				2.190(3)			
	2.179(6)				2.185(3)			
N═C (Å)	1.280(8)	1.274(4)	1.265(6)	1.289(13)	1.271(5)	1.257(3)	1.264(3)	1.243(7)
	1.272(9)		1.245(6)		1.251(5)			1.248(7)
	1.281(8)				1.258(5)			
	1.293(8)				1.265(5)			
U−N═C (deg)	178.9(6)	162.4(3)	174.1(4)	179.0(8)	172.8(3)	176.78(19)	172.48(17)	178.4(4)
	176.5(5)		176.6(4)		176.8(3)			176.3(4)
					169.5(3)			
					171.7(3)			
N−U−N (deg)	109.4(2)	102.40(15)	109.92(15)	112.0(5)	107.51(12)	105.49(11)	111.83(10)	104.8(2)
	107.2(2)				104.02(12)			106.1(2)
ϕ (deg)			49.5	26.8[a]	55.3	60.1	7.0	68.4
			20.4		89.4			73.0
					58.7			
					53.7			

[a] The $[-N{=}C(CH_3)(4\text{-}F\text{-}C_6H_4)]^-$ ligands of this complex are disordered, resulting in only an estimated twist angle for this complex. The value was obtained by averaging the values of the various disordered components. The twist angle for the analogous Th complex $(C_5Me_5)_2Th[-N{=}C(CH_3)(4\text{-}F\text{-}C_6H_4)]_2$ (**12**) is 8.4°.[2]

(orthogonal aryl groups). Table 2 lists the interplanar angles (*ϕ*) for complexes **4**, **6**, **7**, and **9**−**11** and reveals two distinct structure types: complexes **6** and **10** do not contain *o*-fluorine atoms and display interplanar angles in the range of $\phi = 7-26.8°$ (small aryl rotation), while **7**, **9**, and **11** each possess two *o*-fluorine atoms and exhibit significantly larger values of $\phi = 53.7-89.4°$ (large aryl rotation). Complex **4** with a single *o*-fluorine substituent has intermediate values of $\phi = 20.4$ and 49.5°.

For the $6d^05f^0$ $(C_5Me_5)_2Th[-N{=}C(CH_3)(Ar_F)]_2$ complexes possessing two *o*-fluorine atoms and consequently large interplanar (*ϕ*) angles (Ar_F = 2,6-F_2-C_6H_3, 2,4,6-F_3-C_6H_2, or C_6F_5), significant perturbations to electronic structure were observed. Similar electronic structure perturbations might be expected to occur in the isostructural $6d^05f^2$ $(C_5Me_5)_2U[-N{=}C(CH_3)(Ar_F)]_2$ complexes **7**, **9**, and **11**, which also possess large *ϕ* angles. The ground $6d^05f^2$ configuration of the uranium bis(ketimide) complexes provides several more spectroscopic handles to survey the impact of this ketimide ligand rotation on U^{IV} electronic structure. Interestingly, the effect can be qualitatively observed by ^{1}H NMR spectroscopy. All of the complexes **1**−**11** exhibit shifted ^{1}H NMR resonances due to the paramagnetism of the U^{IV} ion (see the Supporting Information). For **4**−**6**, **8**, and **10**, the ketimide aryl proton resonances were significantly broadened at room temperature (298 K) and definitive assignments of these chemical shifts could only be made using variable-temperature (363−388 K) NMR experiments. In contrast, these ketimide aryl protons were easily observed at room temperature for complexes **7** and **9**, which both possess large aryl rotations and interplanar angles ($\phi = 53.7-89.4°$) at room temperature.

In a comparison of the ^{1}H NMR aryl resonances between the sets of complexes **4**−**6**, **8**, and **10** versus **7** and **9**, there should be no significant change in the paramagnetic shift and relaxation by the dipolar interaction, based on the solid-state structural data. It can be surmised that the same primary steric interaction that disrupts the conjugation of the ketimide ligand also causes disruption of the orbital pathway for Fermi contact between the U^{IV} ion and aryl protons in **7** and **9**. This is noteworthy because the NMR data demonstrate that the electronic structure effects associated with the rotation of the ketimide aryl groups are operative in solution.

DFT Calculations. The structures of the ground states of **6** and **11** were calculated using DFT approaches. Overall, there is good agreement between the calculated structures

Table 3. Comparison of Calculated and Experimental Geometric Parameters for Complexes **6** and **11**

	$(C_5Me_5)_2U[-N{=}C(CH_3)(4\text{-}F\text{-}C_6H_4)]_2$ (**6**)		$(C_5Me_5)_2U[-N{=}C(CH_3)(C_6F_5)]_2$ (**11**)	
	exptl	calcd	exptl	calcd
R(U−N) (Å)	2.169(9)	2.185	2.199(5), 2.204(5)	2.199
R(N−C) (Å)	1.289(13)	1.275	1.243(7), 1.248(7)	1.263
R(U−$C_5Me_{5(cent)}$) (Å)	2.446, 2.512	2.544	2.499, 2.513	2.518
∠(N−U−N) (deg)	112.0(5)	107.1	104.8(2)	109.5
ϕ (interplanar angle, deg)	26.8[a]	7.5	65.8	63.7

[a] The $[-N{=}C(CH_3)(4\text{-}F\text{-}C_6H_4)]^-$ ligands of this complex are disordered, resulting in only an estimated twist angle for this complex. The value was obtained by averaging the values of the disordered components. The twist angle for the analogous Th complex $(C_5Me_5)_2Th[-N{=}C(CH_3)(4\text{-}F\text{-}C_6H_4)]_2$ (**12**) is 8.4°.[2]

Table 4. Calculated Electronic Properties for Complexes **6** and **11** and the Corresponding Anions $[\mathbf{6}]^-$ and $[\mathbf{11}]^-$ [a]

	relative energy (eV)		net spin		
	vertical	adiabatic	U	N	C
6	0.0	0.0	2.11	−0.11	+0.09
$[\mathbf{6}]^-$	−0.87	−0.95	2.71	−0.09	+0.19
11	0.0	0.0	2.12	−0.09	+0.09
$[\mathbf{11}]^-$	−1.10	−1.24	2.75	−0.08	+0.19

[a] Vertical energies (eV) and spin properties of the neutral and negative ion species are given. Unpaired spin densities are shown for the U metal center and the ketimide C=N atoms calculated at the equilibrium geometries of the negative ions.

and the X-ray diffraction results (Table 3). The calculated U−N bond lengths for **6** and **11** are 2.185 Å [expt = 2.169(9) Å] and 2.199 Å [expt = 2.199(5) and 2.204(5) Å], and the calculated U−$C_5Me_{5(cent)}$ bond lengths are 2.544 Å (expt = 2.446 and 2.512 Å) and 2.499 Å (expt = 2.499 and 2.513 Å), respectively. The major structural difference between the complexes involving the rotation of the fluorinated aryl ring out of the N=C(C_{Me})(C_{ipso}) ketimide plane is well reproduced by the DFT results. For complex **6**, the aryl ring is nearly coplanar (7.5° calcd; ∼28.6° expt), while in complex **11**, the unfavorable steric interactions between the two *o*-fluorine atoms and the methyl group [−N=C(CH_3)] on the ketimide ligand force the aryl ring to be significantly rotated (65.8° calcd; 63.7° expt).

The electronic properties of the neutral complexes **6** and **11** and their corresponding negative ions are summarized in Table 4. Anion calculations were performed to assess the relative agreement between theory and experiment on the U^{IV}/U^{III} redox energies. The ground state of each molecule corresponds to a high-spin $5f^2$ configuration on the U^{IV} center. The DFT results indicate 2.1 unpaired electrons on each metal with minor spin density residing on the C=N atoms of the ketimide ligands. This can be seen clearly by examining the ground-state NOs that correspond to the singly occupied orbitals in Table 5. These orbitals are localized on the U metal center and comprised entirely of 5f character. By contrast, a more complicated interpretation arises from examining the conventional α-spin molecular orbitals (MOs) of the DFT calculations. In this case, the 5f character, also totaling two electrons, was spread out over several of the highest occupied MOs. See the Supporting Information for Mulliken analysis tables for **6**, **11**, and their anions.

As shown in Table 4, the negative ions $[\mathbf{6}]^-$ and $[\mathbf{11}]^-$ are calculated to be stable relative to the neutral species by 0.95 and 1.24 eV, respectively, as gas-phase species without solvent corrections. The greater electron affinity and electron-withdrawing properties of the pentafluorophenyl group in **11** relative to the 4-fluorophenyl group in **6** correlates with the fact that complex **11** is more easily reduced to U^{III} in the electrochemical studies at −2.34 V (**11**) vs −2.64 V (**6**). While the negative ions formally have a $5f^3$ ground-state configuration, some of the unpaired electron density is delocalized onto the organic ligands (Table 4). Roughly 2.7 unpaired electrons reside on the U metal center according to the Mulliken analysis. This can also be seen in the three NOs corresponding to the unpaired electrons for the negative ions, where significant ligand character is evident (Table 5).

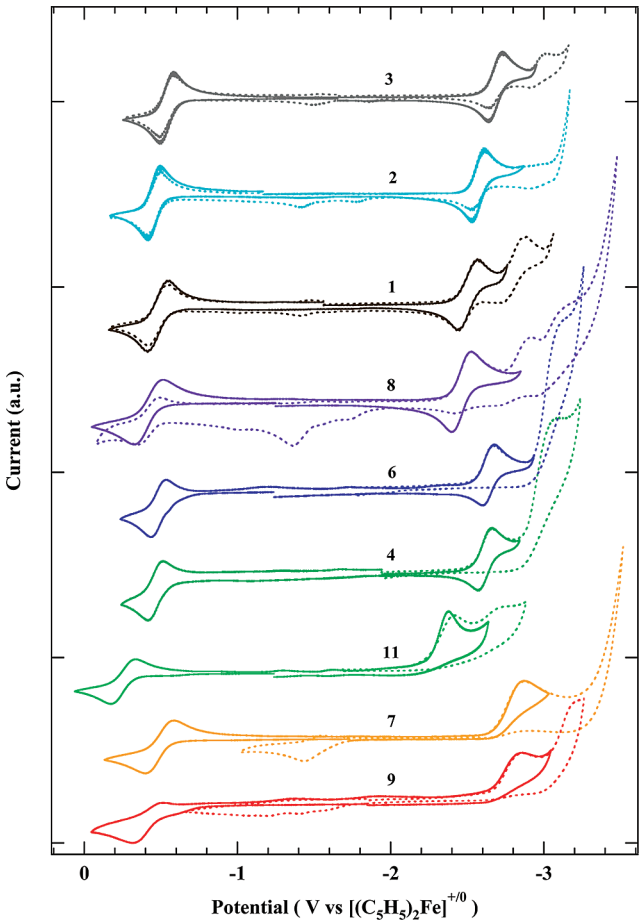

Figure 2. Cyclic voltammograms for ∼5 mM uranium(IV) bis(ketimide) complexes in ∼0.1 M $[Bu_4N][B(C_6F_5)_4]$/THF at room temperature. All scans were collected at 200 mV/s.

Electrochemistry. Room-temperature voltammetric data (cyclic and square wave) were obtained for complexes **1**−**11** in ∼0.1 M $[Bu_4N][B(C_6F_5)_4]$/THF. Typical cyclic voltammetric data are illustrated in Figure 2, and the metrical data

Table 6. Summary of Redox Data for $(C_5Me_5)_2U[-N{=}C(R_1)(R_2)]_2$ Complexes in ~0.1 M $[Bu_4N][B(C_6F_5)_4]$/THF[a]

	R_1	R_2	$E_{1/2}(U^{5+}/U^{4+})$	$E_{1/2}(U^{4+}/U^{3+})$	$E_{1/2}(L)$	$\Delta E_{1/2}(1)$[b]	$\Delta E_{1/2}(2)$[c]
1	C_6H_5	C_6H_5	−0.48 (R)[d]	−2.50(R)[d]	−2.79 (R)[d]	2.02	2.31
2	CH_2Ph	C_6H_5	−0.46 (R)[d]	−2.57 (R)[d]	~−2.9 (R)[d]	2.11	2.4
3	CH_3	C_6H_5	−0.54 (R)[d]	−2.68 (R)[d]	−2.96 (R)[d]	2.14	2.42
4	CH_3	2-F-C_6H_4	−0.46 (R)[d]	−2.62 (R)[d]	−3.02 (I)[f]	2.16	2.56
5	CH_3	3-F-C_6H_4	−0.45 (R)[d]	−2.54 (R)[d]	−2.93 (I)[f]	2.09	2.48
6	CH_3	4-F-C_6H_4	−0.48 (R)[d]	−2.64 (R)[d]	−3.08 (I)[f]	2.16	2.60
7	CH_3	2,6-F_2-C_6H_3	−0.49 (R)[d]	−2.82 (C)[f]	[g]	2.33	
8	CH_3	3,5-F_2-C_6H_3	−0.42 (R)[d]	−2.46 (R)[d]	−2.88 (C), [f] −3.12 (I)[f]	2.04	2.46
9	CH_3	2,4,6-F_3-C_6H_2	−0.43 (R)[d]	−2.80 (I)[f]	−3.18 (I)[f]	2.37	2.75
10	CH_3	3,4,5-F_3-C_6H_2	−0.34 (R)[d]	−2.48 (R)[d]	[g]	2.14	
11	CH_3	C_6F_5	−0.26 (R)[d]	−2.34 (C)[f]	−2.66 (I)[f]	2.08	2.40

[a] Legend: (R) = chemically reversible; (I) = chemically irreversible; (C) = wave becomes reversible at fast scan rates. All values are in volts. $E_{1/2}$ values are versus $[(C_5H_5)_2Fe]^{+/0}$. [b] $\Delta E_{1/2}(1) = E_{1/2}(U^{5+}/U^{4+}) - E_{1/2}(U^{4+}/U^{3+})$. [c] $\Delta E_{1/2}(2) = E_{1/2}(U^{5+}/U^{4+}) - E_{1/2}(L_1)$. [d] $E_{1/2}$ was determined from $(E_{pc} + E_{pa})/2$ at 200 mV/s. [e] $E_{1/2}$ was estimated from $(E_{pc} + E_{pc/2})/2$ at 200 mV/s. [f] $E_{1/2}$ was determined from the peak potential in a square-wave voltammogram. [g] Distinct wave not observed within the available potential window.

from the electrochemical experiments are summarized in Table 6. These voltammetric data are generally consistent with those reported previously for uranium(IV) bis(ketimide) complexes.[1,9,13] In particular, the stabilizing influence of the σ- and π-donating ketimide ligands leads to a ready accessibility of the U^V/U^{IV} redox couple in addition to the more common U^{IV}/U^{III} couple. The ketimide ligands are also sources of reductive redox processes (although some of the fluorinated ketimide ligands have somewhat ambiguous reduction chemistry as described below), as verified by the appearance of essentially identical ligand-based voltammetric behavior in the analogous thorium(IV) metallocene complexes.[1,2,9] These reduction steps are invariably coupled to chemical transformations that render the electron-transfer step(s) irreversible and lead to additional new oxidation features in the voltammograms (dashed-line traces in Figure 2). There is no apparent ketimide ligand-based oxidative electrochemistry. The only other redox processes that can be observed for these complexes in this solvent/electrolyte system are attributed to irreversible pentamethylcyclopentadienyl ($C_5Me_5^-$) ligand-based oxidation common to all of the tetravalent actinide metallocene complexes at approximately +1 V versus $[(C_5H_5)_2Fe]^{+/0}$.[1]

For the majority of the uranium(IV) bis(ketimide) complexes, both of the metal-centered redox transformations (U^V/U^{IV} and U^{IV}/U^{III}) are chemically reversible, as evidenced by the appearance of cathodic and anodic waves for both couples in the cyclic voltammograms (Figure 2). Thus, it is noteworthy that the putative U^{IV}/U^{III} couple for the fluorinated ketimide complexes **7**, **9**, and **11** shows signs of irreversible behavior (Figure 2). Note that these are the three complexes that possess two *o*-fluorine atoms on the ketimide aryl group and exhibit the structural distortion discussed above, which results in disruption of conjugation through the ketimide ligand. The ultimate origin of this seemingly irreversible behavior is at present unknown, but preliminary DFT calculations do indicate a potential structural change in the ketimide ligand upon reduction for complex **11** that is not

Table 5. NOs Corresponding to Singly Occupied Orbitals in Complexes **6**, **11**, and Their Corresponding Anions

NOs	**6**	**[6]$^-$**	**11**	**[11]$^-$**
NO-1	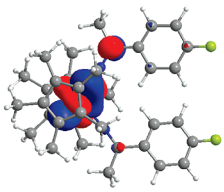	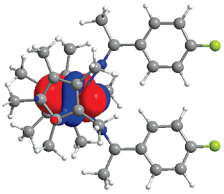	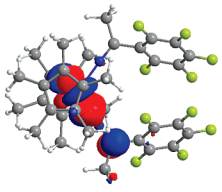	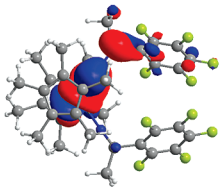
NO-2	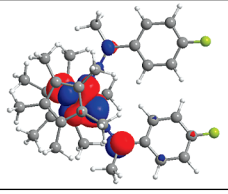	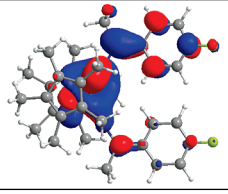	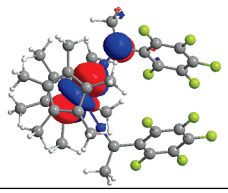	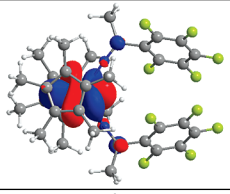
NO-3		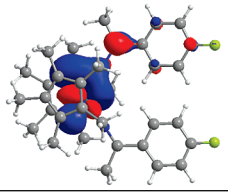		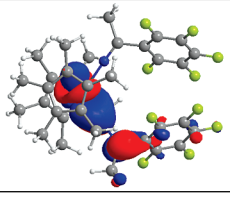

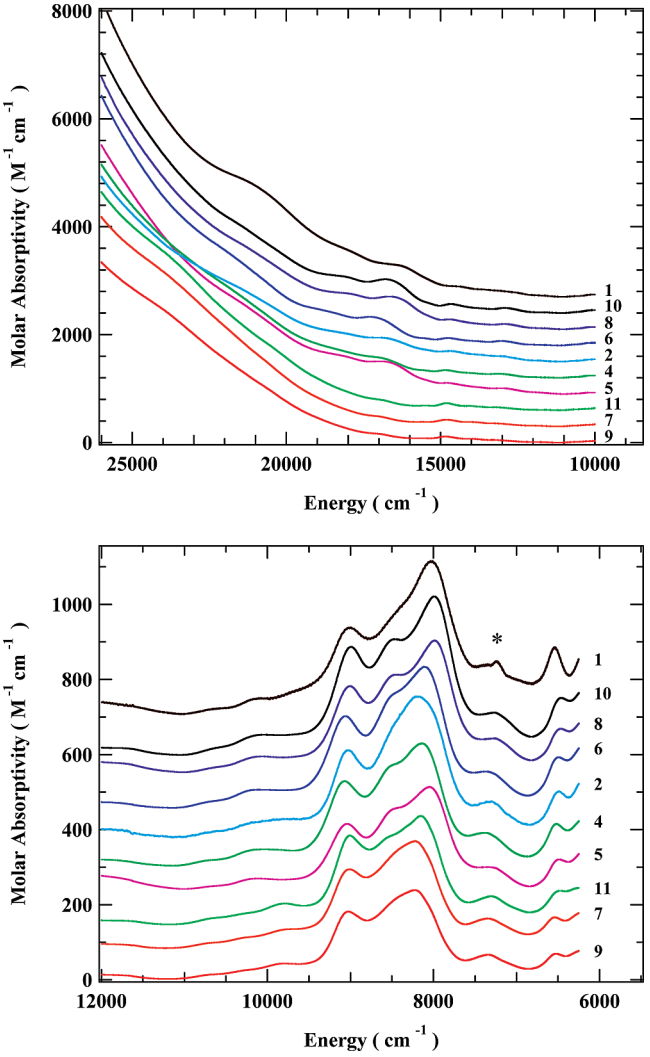

Figure 3. UV−visible (top panel) and near-IR (bottom panel) spectra for uranium(IV) bis(ketimide) complexes in a toluene solution at room temperature. Spectra are offset for clarity; $\epsilon \cong 0$ at 11 000 cm^{-1} for all spectra. The asterisk denotes a small contribution from a solvent vibrational band that was incompletely subtracted.

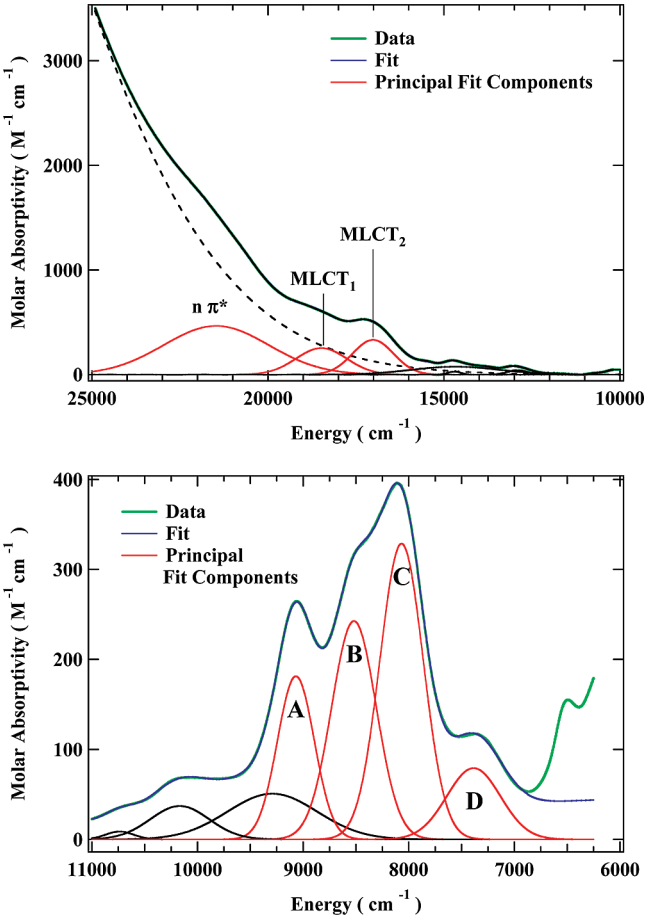

Figure 4. Examples of spectral deconvolutions of the UV−visible (top panel) and near-IR (bottom panel) regions of the electronic spectra for **6** in a toluene solution at room temperature. Labels on component fit bands correspond to those listed in Table 7.

seen for complex **6**. Additional theoretical and experimental studies of this redox behavior are underway and will be reported elsewhere.

A final interesting observation from these electrochemical data is the consistency in the separation between the two metal-based redox processes across this range of ligands [$\Delta E_{1/2}(1)$ in Table 6]. This same observation was made previously for a range of $(C_5Me_5)_2U^{IV}LL'$ complexes, where L and L′ are ligands capable of stabilizing the U^V oxidation state through both σ- and π-bonding interactions (e.g., ketimides, hydrazonates, and imides).[1] In this prior study, the average $\Delta E_{1/2}(1)$ value was 2.1 V. Here, the average value for all 11 bis(ketimide) complexes is 2.15 ± 0.03 V. Thus, these new fluorinated ketimide complexes preserve this interesting trend in the redox energetics of these principally metal-based redox transformations.

Electronic Absorption Spectroscopy. The electronic absorption spectral data for complexes **1**, **2**, and **4**−**11** are illustrated in Figure 3. These data have been broken out into the UV−visible region (top panel, Figure 3) and the near-IR region (bottom panel, Figure 3) to better compare the spectral properties of these complexes and facilitate further discussion. Note in particular that there is good qualitative correlation among the near-IR spectral data for all 10 complexes but some apparent greater variability in behavior in the UV−visible spectral region. All spectral data were successfully fit in both the UV−visible and near-IR regions using a sum of Gaussian bands, as illustrated for **6** in Figure 4. A Gaussian band was also required to account for the low-energy tail of the unresolved high-energy feature in the UV−visible region, as indicated by the dashed line (Figure 4). The metrical parameters derived from these fits for the principal bands in each region are compiled in Table 7. Some summary statistical data have been included for these metrical parameters. These statistics have no intrinsic meaning but are simply provided to illustrate the strong correlation in the electronic transitions among these 10 complexes.

The bands observed in the near-IR region can be assigned unambiguously to intraconfiguration f−f ligand-field transitions on the basis of their *relatively* low oscillator strengths and their energy range, which are consistent with a $5f^2$ U^{IV} ion. The rather broader, less distinct features in the UV−visible region provide a greater challenge in assignment and

Table 7. Summary of Electronic Spectral Data for $(C_5Me_5)_2U[-N{=}C(R_1)(R_2)]_2$ Complexes in a Toluene Solution at Room Temperature

	complex		electronic transition energy (E) and oscillator strength (f)													
			$n\pi^*$		$MLCT_1$		$MLCT_2$		$f-f_A$		$f-f_B$		$f-f_C$		$f-f_D$	
	R_1	R_2	E (cm^{-1})	f ($\times10^3$)	E (cm^{-1})	f ($\times10^3$)	E (cm^{-1})	f ($\times10^3$)	E (cm^{-1})	f ($\times10^6$)	E (cm^{-1})	f ($\times10^6$)	E (cm^{-1})	f ($\times10^6$)	E (cm^{-1})	f ($\times10^6$)
1	C_6H_5	C_6H_5	20658	13.7	17862	2.8	16249	2.4	9044	190	8278	1040	7980	283	7283	71
2	CH_2Ph	C_6H_5	21318	10.9	18122	1.5	16708	1.7	9050	228	8326	932	7999	307	7331	137
4	CH_3	2-F-C_6H_4	21739	14.1	18138	1.5	16834	0.98	9077	410	8560	505	8101	671	7399	191
5	CH_3	3-F-C_6H_4	20955	8.5	18046	2.7	16605	1.7	9053	229	8492	505	8012	539	7351	180
6	CH_3	4-F-C_6H_4	21470	7.5	18482	2.0	17015	2.1	9069	342	8519	556	8069	731	7386	217
7	CH_3	2,6-F_2-C_6H_3	20822	2.4	18723	3.0	16900	0.15	9056	206	8445	832	8110	202	7344	100
8	CH_3	3,5-F_2-C_6H_3	20899	7.9	17859	1.9	16438	2.4	9028	263	8479	690	7962	649	7314	233
9	CH_3	2,4,6-F_3-C_6H_2	20897	1.9	19056	3.5	16923	0.14	9056	166	8427	672	8120	152	7343	79
10	CH_3	3,4,5-F_3-C_6H_2	20846	5.7	18037	1.6	16604	2.6	9017	292	8486	795	7964	729	7309	216
11	CH_3	C_6F_5	20562	6.8	18374	2.7	16847	0.15	9044	203	8463	945	8082	199	7301	79
	av		21017	7.9	18270	2.3	16712	1.4	9049	253	8448	748	8040	446	7336	150
	std dev		118	1.3	123	0.2	76	0.3	6	24	27	61	20	76	12	20

require consideration of multiple lines of evidence as discussed below.

A useful starting point for the assignment of the UV−visible electronic transitions in these uranium bis(ketimide) complexes is a comparison of this spectral region for the analogous thorium bis(ketimide) complex $(C_5Me_5)_2Th[-N{=}C(CH_3)(4\text{-}F\text{-}C_6H_4)]_2$ (**12**) and the uranium bis(alkyl) starting material $(C_5Me_5)_2U(CH_3)_2$. Such a comparison is provided in Figure 5 for **6**. The features of particular interest in these spectral data are indicated by arrows in Figure 5, and these are among the ones that distinguish complex **6** from its thorium analogue (**12**) and $(C_5Me_5)_2U(CH_3)_2$.

Inasmuch as there are no readily accessible valence orbitals on the metal in the thorium bis(ketimide) complex, the observed UV−visible transitions in complex **12** must be ligand-based (ketimide and/or C_5Me_5).[17] Furthermore, the isostructural uranium bis(ketimide) complexes should possess the same transitions at similar energies and with comparable intensities because the ligand sets are identical. The distinct band in the Th complex **12** at ~22 000 cm^{-1} (Figure 5) has been assigned to a set of two nearly degenerate ketimide-based $p_N \rightarrow \pi^*_{C=N}$ transitions ($n\pi^*$) that are relatively weak because although spin-allowed they are orbitally forbidden.[2] The uranium bis(ketimide) complexes all exhibit one or two well-defined shoulders in this same energy range and with approximately the same intensity (Figures 3 and 5) that are assigned to these same electronic transitions. (Data for only the lowest-energy $n\pi^*$ band are provided in Table 7.)

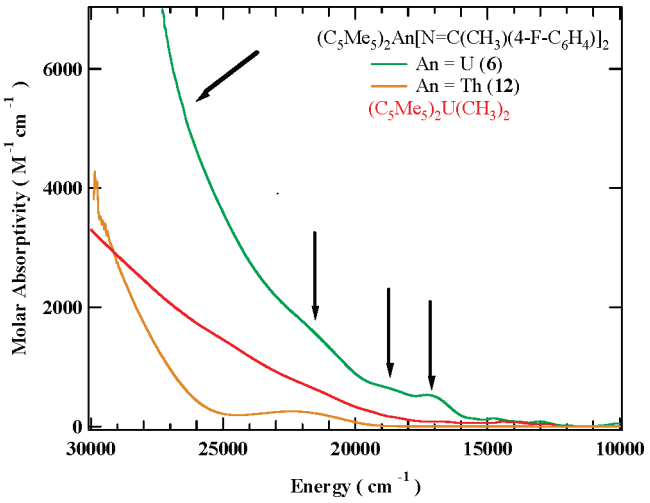

Figure 5. Comparison of the UV−visible spectra of **6**, **12**, and $(C_5Me_5)_2U(CH_3)_2$ in a toluene solution at room temperature.

As illustrated in Figure 5, the two lower-energy bands identified in the uranium bis(ketimide) spectrum have no analogues in the spectra of either the thorium bis(ketimide) complex **12** or the uranium bis(alkyl) complex $(C_5Me_5)_2U(CH_3)_2$. This is the spectral region that engendered the greatest resonance enhancement in the Raman vibrational bands localized on the ketimide ligand of **1**.[5] On the basis of this observation, these electronic bands were assigned to metal (U) → ligand (ketimide π^*) CT (MLCT) transitions because such a transition should have a large Franck−Condon distortion in the ketimide modes between the ground and MLCT excited states.[5] This same set of electronic bands is observed in all of the uranium bis(ketimide) complexes reported here (Figure 3), and the MLCT assignment is still preferred based on the Raman result and the following additional considerations. First, the electrochemical data clearly show that the ketimide ligands possess accessible acceptor orbitals, while the metal center can be readily oxidized. These results establish the thermodynamic feasibility for an MLCT optical process.[18] Second, the energy of these optical bands is intermediate between those of the ligand-field bands (bottom panel, Figure 3) and the ketimide-localized $n\pi^*$ bands. DFT calculations indicate that the energy of the 5f orbital manifold in the uranium bis(ketimide) complexes is intermediate between those of the ketimide nonbonding N p orbitals and the ketimide C=N π^* orbitals (see, for example, Figure 2 in ref 19). Although time-dependent DFT calculations are unable to predict the energies of transitions associated with the open-shell $5f^2$ orbital manifold, the orbital energies serve as a rough basis for predicting the relative transition energies. In particular, the energy of the $5f_U \rightarrow$ ketimide $\pi^*_{C=N}$ MLCT transition should correspond approximately to the energy separation between the occupied 5f orbital and the unoccupied ketimide $\pi^*_{C=N}$

(17) Manuta, D. M.; Lees, A. J. *Inorg. Chem.* **1986**, *25*, 3212.
(18) Lever, A. B. P., Dodsworth, E. S., Solomon, E. I., Lever, A. B. P., Eds.; John Wiley & Sons, Inc.: New York, 1999; Vol. 2.
(19) Clark, A. E.; Martin, R. L.; Hay, P. J.; Green, J. C.; Jantunen, K. C.; Kiplinger, J. L. *J. Phys. Chem. A* **2005**, *109*, 5481.

orbital so long as the coulomb (J) and exchange (K) integral energies do not make too large a contribution to the transition energy. The magnitudes of J and K scale with the extent of orbital overlap and should therefore be relatively small for overlap of 5f and ligand π^* orbitals.[18] Third, while the intensity and line widths of these bands may seem anomalously small for fully dipole-allowed MLCT bands (compared to d$-\pi^*$ transitions in transition-metal complexes), it should be noted that CT intensities also scale with the extent of orbital overlap between participating metal and ligand orbitals. Here, too, the overlap between the 5f and ligand $\pi^*_{C=N}$ orbitals, while believed to be unusually large for actinide systems, is small in comparison to d orbital overlap with ligand orbitals in transition-metal complexes. In fact, the observed extinction coefficients in these bands for the uranium bis(ketimide) complexes ($\epsilon = \sim 250-300$ M^{-1} cm^{-1} for **6**; Figures 3 and 5) are significantly larger than those found for the paradigmatic $p_{oxygen} \rightarrow 5f_U$ ligand-to-metal CT transition in typical UO_2^{2+} complexes possessing strong metal$-$ligand covalent bonding ($\epsilon = \sim 50-100$ M^{-1} cm^{-1}; see, for example, Figure 4 in ref 20). Finally, it is possible that the two bands ($MLCT_1$ and $MLCT_2$) are simply resolved vibronic components of a transition to a single MLCT excited state. The spacing between these two bands (Table 7) is in the range of $\sim 1300-1700$ cm^{-1} for the entire series (i.e., corresponds to a typical mid-IR vibrational mode), which would be consistent with a ketimide ligand-localized vibrational mode that undergoes a Franck$-$Condon distortion between the ground and MLCT excited states, as was already demonstrated in the resonance Raman data.

A final consideration in the UV$-$visible spectral region for the uranium bis(ketimide) complexes is the substantial intensity in the unresolved high-energy band relative to that of $(C_5Me_5)_2U(CH_3)_2$ (Figure 5). As has been noted previously, the methyl ligands in $(C_5Me_5)_2U(CH_3)_2$ only interact with the metal center in a σ-donor fashion.[1] Because there are no low-lying methyl ligand-based orbitals available to participate in ligand-based and/or CT transitions, the UV$-$visible spectral region of this complex should be dominated by metal-based interconfiguration and perhaps C_5Me_5-metal-derived electronic transitions. To a first approximation, these same metal-based ($5f^2 \rightarrow 5f^16d^1$) and/or $C_5Me_5 \leftrightarrow$ metal CT transitions should be present in the uranium bis(ketimide) complexes with approximately the same energy and intensity as in the bis(alkyl) species $(C_5Me_5)_2U(CH_3)_2$. Pentamethylcyclopentadienyl ligand-localized $\pi-\pi^*$ transitions are also possible, but these should be roughly the same in the Th and U complexes and, based on the data for the Th complex, occur at higher energy than is shown in Figure 5. A $5f^2 \rightarrow 5f^16d^1$ assignment for this unresolved band in the uranium bis(ketimide) complexes seems potentially attractive because such transitions should have large oscillator strengths and fairly broad bandwidths. Previous studies of classical U^{IV} coordination complexes place this transition at higher energy;[21−25] however, the stronger σ- and π-interactions of the ketimide ligands with the metal center may stabilize some subset of metal 6d orbitals as well, thereby lowering the energy of the interconfiguration transition relative to that in, for example, the $(C_5Me_5)_2U(CH_3)_2$ complex. The ultimate uncertainty in assigning this transition is exacerbated by the much greater potential for mixing of excited states in these ketimide complexes as a result of more favorable metal$-$ligand orbital energy matching and greater metal$-$ligand bonding interactions.

As noted above, there is a remarkable degree of consistency in the f$-$f spectral region for all of the uranium bis(ketimide) complexes considered in this study (bottom panel, Figure 3). As seen in the summary statistical data in Table 7, the standard deviations in the energies of the four principal f$-$f bands among this sample population is only $\sim 5-25$ cm^{-1} (i.e., comparable to the spectral resolution in this wavelength range). However, there is some significant variability in the oscillator strengths of these bands across this series of complexes suggestive of an origin in some component of the electronic structure of these complexes. Variations in both intensities and energies resulting from changes in ligand- or crystal-field perturbations are typically correlated according to the nephelauxetic effect.[26] Changes in the magnitude of the ligand field across the series of ketimide ligands studied here appear to be manifest in the magnetic susceptibility data, but the observed intensity changes in the optical spectral data for these f$-$f bands are believed to have a different origin. In our previous study of uranium(IV) metallocene complexes containing a variety of ligand types, we suggested that the f$-$f intensities in the ketimide complexes in particular exhibited substantial enhancement relative to the values found in complexes of simple σ-donor ligands such as halides and alkyls.[1] To provide some quantitative basis for this intensity enhancement, note that the oscillator strengths in the more intense f$-$f bands of $(C_5Me_5)_2U(CH_3)_2$ and the bis(hydrazonato) complex $(C_5Me_5)_2U[\eta^2\text{-}(N,N)\text{-}CH_2Ph-N-N{=}CPh_2]_2$ (**13**) are 33×10^{-6} (band at 10 930 cm^{-1}) and 47×10^{-6} (band at 10 100 cm^{-1}), respectively.[1] In contrast, the oscillator strengths in the more intense f$-$f bands of the uranium bis(ketimide) complexes average $\sim 400 \times 10^{-6}$ for the four bands identified in Table 7 over the entire series of complexes.

Studies of the intensity enhancement for parity-forbidden ligand-field (d$-$d) optical transitions in transition-metal complexes were expected to provide a framework for discerning the mechanism for the observed intensity enhancement in the f$-$f ligand-field bands for the uranium bis(ketimide) complexes. The most common enhancement mechanism for d$-$d transitions is by a Herzberg$-$Teller

(20) Clark, D. L.; Conradson, S. D.; Donohoe, R. J.; Keogh, D. W.; Morris, D. E.; Palmer, P. D.; Rogers, R. D.; Tait, C. D. *Inorg. Chem.* **1999**, *38*, 1456.
(21) Krupa, J. C. *J. Alloys Compd.* **1995**, *225*, 1.
(22) Krupa, J. C. *J. Solid State Chem.* **2005**, *178*, 483.
(23) Godbole, S. V.; Page, A. G.; Sangeeta Sabharwal, S. C.; Gesland, J. Y.; Sastry, M. D. *J. Lumin.* **2001**, *93*, 213.
(24) Poturaj-Gutniak, S.; Taube, M. *J. Inorg. Nucl. Chem.* **1968**, *30*, 1005.
(25) Barandiaran, Z.; Seijo, L. *J. Chem. Phys.* **2003**, *118*, 7439.
(26) Lever, A. B. P. *Inorganic Electronic Spectroscopy*, 2nd ed.; Elsevier: Amsterdam, The Netherlands, 1984.

process that mixes energetically close CT states into the ligand-field states.[26] Given the energetic proximity of the MLCT states in the uranium bis(ketimide) complexes, it was expected that these states could provide the agency for the observed ~10-fold intensity enhancements relative to those seen in the bis(alkyl) complexes noted above by mixing some CT character into the f−f state. However, if this were the operative mechanism, there should be an approximately linear correlation between the oscillator strength of the f−f band and that of the CT band involved in the mixing because the matrix element for the transition moment between the perturbed f orbital states contains linear terms in the CT transition moment matrix element. No such correlation has been observed for any of the f−f bands in relation to either of the MLCT bands or the ligand-based $p_N \rightarrow \pi^*_{C=N}$ bands in the data in Table 7. Here, however, any trends in intensity stealing from the higher lying MLCT and ligand-based states could be masked by competing influences such as the unfavorable steric factors noted for **7**, **9**, and **11** that might artificially suppress (or enhance) the intensities of the CT and/or ligand-based transitions. Thus, the apparent large f−f intensity enhancement remains a challenge to explain.

Magnetic Susceptibility. The magnetic response of compounds **4**−**11** was measured between 350 and 2 K to evaluate changes in the electronic structure based on different ketimide groups. Before comparison of the series of compounds, it is useful to discuss the general magnetic behavior of the U^{IV} ion to establish expectations for comparison between complexes. Actinide ions resist simple, precise interpretation of their magnetic behaviors for the usual reasons that have been discussed extensively elsewhere.[27,28] The primary consideration is that the magnitude of the spin−orbit coupling is equal to or larger than the interelectron repulsion resulting in terms from excited-state configurations that contribute to the ground-state term. This results in an admixture, making the quantum number J an ineffective reckoning for the accounting of states. The reality of the situation for many U^{IV} complexes is that the admixture turns out to be small enough (<10% $6d^15f^1$ contribution to the ground-state $6d^05f^2$ configuration) that Russell−Saunders coupling *can* be used successfully,[29] especially in the context of a series of complexes such as those under investigation here.

Using the Russell−Saunders coupling scheme, treatment of the U^{IV} ion results in a ground-state $^3H_4$ term analogous to the Pr^{III} ion. However, because the ground-state $^3H_4$ term is split by crystal-field energies larger than the thermal energies kT achieved in these experiments, the susceptibility data will never reach the high-temperature Curie value (or even ±10%) for a $J = 4$ term of $C = 1.60$ emu K mol^{-1} (3.58 μ_B). Also, because of larger 5f and ligand orbital overlap, these crystal-field splittings in U complexes should

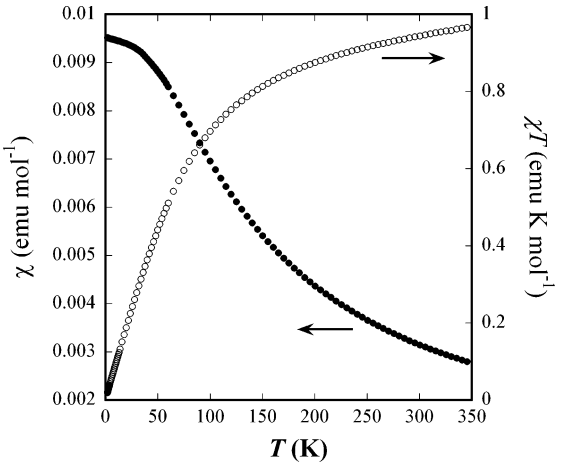

Figure 6. Magnetic susceptibility of **11** from 2 to 350 K.

be more sensitive to ligand variation than their lanthanide counterparts. With this electronic structure framework in mind, the following expectations for magnetic susceptibility measurements of **4**−**11** can be applied: (1) J is an effective quantum number and the $^3H_4$ ground-state term for U^{IV} $5f^2$ will be used; (2) the $^3H_4$ term in a low-symmetry crystal field (C_{2v}) completely lifts its degeneracy, yielding $2J + 1 = 9$ singlet states; (3) appreciable magnetic moments are only obtained with a population of more than one crystal-field state due to an orbital (L) component; (4) perturbations on the electronic structure observed in the magnetic response will be manifest in the ligand-field manifold.

The response of a representative uranium(IV) bis(ketimide) complex, **11**, is shown in Figure 6. This compound shows typical magnetic behavior for a U^{IV} $5f^2$ ion with a nominal $^3H_4$ ground-state term and attains a χT product of 0.97 emu K mol^{-1} (2.78 μ_B) at 350 K, consistent with reported values for U^{IV} complexes[27,29−33] and only coincidentally close to the expected value of 1.0 emu K mol^{-1} for a simple $S = 1$, $g = 2$ Curie paramagnet. Compared to a $J = 4$ Curie paramagnet, complex **11** exhibits a small but measurable temperature dependence. As seen in Figure 6, χ versus T increases slightly with decreasing temperature until it reaches ~30 K, where it becomes temperature-independent. This temperature dependence is reflected in χT versus T by the monotonic decrease with temperature and approach to zero at 2 K. The broad trend of χ versus T indicates that the first crystal-field excited state is being thermally depopulated over the temperature range examined. Previous reports have shown similar U^{IV} magnetic behavior that was assumed to result from an excited-state triplet contribution;[34] however, in the low symmetry of **11**, the first excited state is also a singlet. Therefore, the temperature-dependent paramagnetism must arise from an orbital contribution that is only manifest with the thermal population of multiple states. Furthermore,

(27) Boudreaux, E. A.; Mulay, L. N. *Theory and Applications of Molecular Paramagnetism*; Wiley: New York, 1976.
(28) Marks, T. J., Fragala, I. L., Eds. *NATO Advanced Science Institutes Series C: Mathematical and Physical Sciences*; NATO: Dordrecht, The Netherlands, 1985; Vol. 155.
(29) Grunzweig-Genossar, J.; Kuznietz, M.; Friedman, F. *Phys. Rev.* **1968**, *173*, 562.
(30) Gans, P.; Marriage, J. *J. Chem. Soc., Dalton Trans.* **1972**, 46.
(31) Karraker, D. G.; Stone, J. A. *Inorg. Chem.* **1972**, *11*, 1742.
(32) Salmon, L.; Thuery, P.; Riviere, E.; Miyamoto, S.; Yamato, T.; Ephritikhine, M. *New J. Chem.* **2006**, *30*, 1220.
(33) Castro-Rodriguez, I.; Meyer, K. *Chem. Commun.* **2006**, 1353.
(34) Hirose, M.; Miyake, C.; Du Preez, J. G. H.; Zeelie, B. *Inorg. Chim. Acta* **1988**, *150*, 293.

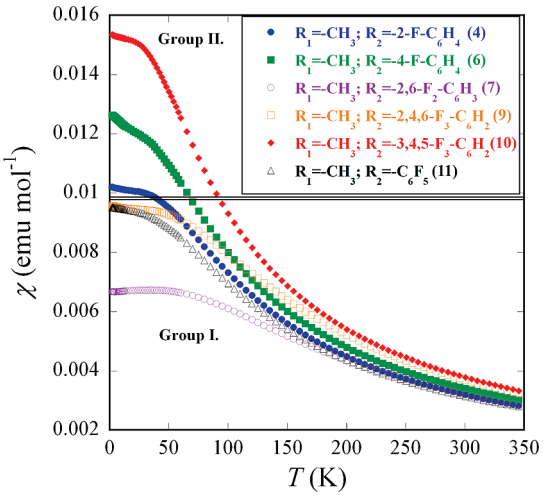

Figure 7. Temperature-dependent magnetic susceptibility data for **4**, **6**, **7**, and **9**−**11** from 2 to 350 K.

the temperature-independent value attained at low temperature is a result of temperature-independent paramagnetism (TIP) derived from admixing of low-lying crystal-field excited states into the ground state.

In the collection of the magnetic data for **4**−**11**, we encountered difficulties in obtaining reproducible data for χ versus T, especially in the low-temperature regime <30 K. We attribute this to paramagnetic impurities that contribute a Curie tail to the data, especially in the context of the small moments that are being measured in this temperature regime. The result of the Curie tail is a masking of the low-temperature TIP behavior. We were able to overcome this issue by using pulverized, dry samples of single crystals for measurements. Such samples could not be obtained for compounds **5** and **8**, which are included as Supporting Information with their acknowledged Curie tails. The χ versus T data for compounds **4**, **6**, **7**, and **9**−**11** are shown in Figure 7. Several of these data sets, especially those for **6**, exhibit small Curie tails, which do not affect the outcome of the comparison within this data. Interestingly, a comparison of these data sets reveals marked differences between their low-temperature responses.

Figure 7 shows the low-temperature magnetic responses for compounds **4**, **6**, **7**, and **9**−**11**, which are different depending on the identity of the fluorinated aryl ketimide substituent. This indicates that, by changing the ligands, the electronic fine structure of the crystal-field manifold of these complexes is perturbed. Furthermore, the complexes can be roughly segregated into two groups based on the magnitude of their low-temperature magnetic moments. Group I consists of compounds **7**, **9**, and **11**, while group II consists of **4**, **6**, and **10**. The distinction between the groups is consistent with the structural change noted previously upon ortho fluorination of the aryl rings on the ketimide ligands. Group I, possessing two *o*-fluorine atoms on the ketimide aryl group, exhibits smaller TIP values at low temperature, indicating a larger energy separation between the ground and TIP-admixed excited states, while group II has these excited states lower in energy. On the basis of the theoretical treatment that shows that ortho fluorination disrupts the $-N{=}C(CH_3)(Ar_F)$ conjugation at the N=C unit, the segregation of these groups in the magnetic behavior is a manifestation of the weaker ketimide ligand basicity of group II versus group I. In concert with the suite of electrochemical and spectroscopy data collected on these systems as well as the theoretical treatment, we attribute the differences in low-temperature magnetic response to ligand-field perturbation of the U^{IV} paramagnetic states. Importantly, these studies provide complementary data because the energetic differences between complexes manifest in the magnetic data are on the order of 10^1-10^2 cm^{-1}, readily discernible in their magnetic susceptibilities but too small to be manifest in the ambient temperature optical data discussed above. The differences between complexes arise from the combination of the primary effect of fluorination at the ortho positions and the secondary effect of the extent and position of the fluorination.

The ultimate observation that can be made from the sum of the magnetic data is that complexes with rotated aryl groups result in a larger separation between the ground and excited states responsible for the TIP contribution in their low-temperature magnetic response. This larger state separation results in a smaller low-temperature χ versus T response (and magnetic moment) for complexes with rotated aryl groups.

Conclusions

The series of fluorinated uranium ketimide complexes on which we report here have provided valuable additional insight into the hallmarks of covalent bonding interactions in early actinide ketimide chemistry. Structural chemistry, experimental data, and DFT have come together to provide a uniform description of these systems that is highlighted by (1) stabilization of multiple metal oxidation states (U^{III}, U^{IV}, and U^{V}), (2) the appearance of new CT and interconfiguration electronic transitions that are classically the domain of transition-metal chemistry, (3) enhanced intensities in the intraconfiguration (f−f) transitions, and (4) variable degrees of TIP at low temperature. All of these elements are a reflection of the strong metal−ligand bonding interactions sustained by the ketimide ligands and varied in response to the different degrees of fluorination of the ketimide aryl group. Furthermore, the impact of the unfavorable steric interactions due to the *o*-fluorine atoms in **7**, **9**, and **11** that lead to a structural distortion and disruption of the orbital delocalization in the ketimide ligand is evidenced in nearly every line of experimental data. The effects are most pronounced in the loss of reversibility of the U^{IV}/U^{III} redox transformation and the extent of excited-state admixture within the symmetry-split $^3H_4$ manifold that leads to the observed TIP at low temperature. Coupled with our recent studies of the analogous thorium fluoroketimide complexes, we have established an exciting new link between the molecular electronic structural properties of the early actinides and those of the d-block metals and identified some as-yet unresolved issues. These studies will certainly provide the motivation for future exploration of covalency and metal−ligand bonding in this fascinating class of complexes.

Acknowledgment. For financial support of this work, we acknowledge the LANL Glenn T. Seaborg Institute for Transactinium Science (Postdoctoral fellowships to E.J.S. and P.Y.), LANL (Director's and Frederick Reines Postdoctoral Fellowships to E.J.S.), the LANL Laboratory Directed Research & Development Program, and the Division of Chemical Sciences, Office of Basic Energy Sciences, Heavy Element Chemistry program. We thank Kimberly C. Jantunen for executing preliminary reactions. This work was carried out under the auspices of the National Nuclear Security Administration of the U.S. Department of Energy at Los Alamos National Laboratory under Contract DE-AC52-06NA25396.

Supporting Information Available: Details of materials, synthetic and crystallographic experimental methods, tables of Mulliken analysis results for **6**, **11**, and their anions, magnetic susceptibility data for **5** and **8**, tables with bond lengths and angles for the structures of **4**, **6**, **7**, **9**, **10**, and **11**, and thermal ellipsoid plots of **4**, **6**, **7**, and **11**. This material is available free of charge via the Internet at http://pubs.acs.org.

IC700455B